Lawrence Berkeley Laboratory
UNIVERSITY OF CALIFORNIA

Materials & Molecular
Research Division

HIGH-TEMPERATURE THERMODYNAMIC ACTIVITIES OF ZIRCONIUM IN PLATINUM ALLOYS DETERMINED BY NITROGEN-NITRIDE EQUILIBRIA

David Alan Goodman
(Ph.D. thesis)

May 1980

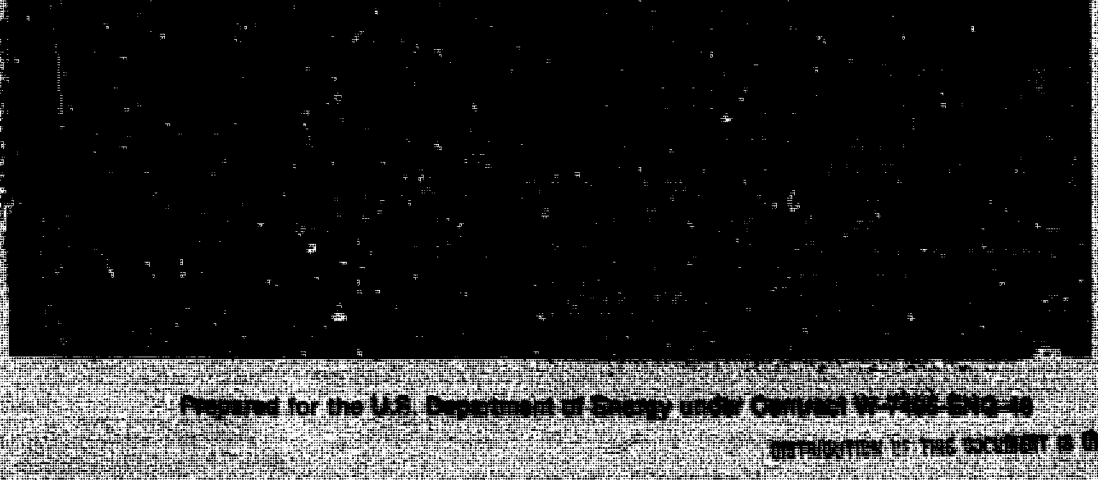

Prepared for the U.S. Department of Energy under Contract W-7405-ENG-48

High-Temperature Thermodynamic Activities of Zirconium in Platinum Alloys Determined by Nitrogen-Nitride Equilibria

by

David Alan Goodman

Materials and Molecular Research Division, Lawrence Berkeley Laboratory
and Department of Chemistry, University of California
Berkeley California 94720

Abstract

A high-temperature nitrogen-nitride equilibrium apparatus is constructed for the study of alloy thermodynamics to 2300°C. Zirconium-platinum alloys are studied by means of the reaction

$$9ZrN + 11Pt \rightarrow Zr_9Pt_{11} + \tfrac{9}{2}N_2.$$

Careful attention is paid to the problems of diffusion-limited reaction and ternary phase formation. The results of this study are

$$a_{Zr}^{1985^oC} = 2.4\times10^{-4} \quad \text{in } Zr_9Pt_{11}$$

and

$$\Delta G^o_{f,1985^oC} \quad Zr_9Pt_{11} \leq -16.6 \text{ kcal/g atom.}$$

These results are in full accord with the valence bond theory developed by Engel and Brewer; this confirms their prediction of an unusual interaction of these alloys.

L.B.L. 10633

High-Temperature Activities of Zirconium in Platinum Alloys Determined by Nitrogen-Nitride Equilibria

David Alan Goodman

Ph.D. Thesis

U. S. Department of Energy
Contract No. W-7405-Eng-48

to my loving parents

Table of Contents

Preface

The metal needs and energy shortages predicted at the end of the century have spurred renewed interest in predictive models of inorganic materials' behavior. Government and industry planners are developing processes and devices to solve the energy problem, but they lack the materials to implement their designs. For instance, coal gasification plants, costing hundreds of millions of dollars, suffer significant corrosion after operating for six months. The traditional methods applied for testing the suitability of materials has not met the demand; predictive models are necessary to anticipate the needs of research and industry. These models will provide an avenue to anticipate problems, cut the cost factor, and provide materials in advance of the need.

The physical scientist plays a vital role in the synthesis of new materials primarily because of his knowledge of the forces acting between atoms; the development of models that relate bulk properties of materials to their atomic structure is a fascinating process.

The goal of this thesis is to contribute to the development of our understanding of the electronic interactions that hold matter together by studying the thermodynamic properties of Lewis-acid-base transition metal alloys. High-temperature thermodynamic activities in zirconium-platinum, zirconium-iridium-platinum, and zirconium-silicon-platinum alloys have been determined. Chapter I is an introduction to the work. Chapter II is a sketch of the Engel-Brewer theory of phase stability; the choice of alloy systems is justified in this chapter. Chapter III presents pertinent data from the literature.

The apparatus and procedures of the experimental work are described in Chapter IV. Chapter V discusses the sources of error. The results and discussion are presented in Chapter VI. Suggestions for future research are given in Chapter VII.

Acknowledgements

My sincerest thanks go to Professor Leo Brewer for the knowledge, confidence, and encouragement he provided throughout the course of this work.

I am thankful to Karen Krushwitz and Harry Weeks, who have been generous with their help when it was sorely needed.

Dr. Gary Bullard, Dr. John Wang, Nathan Jacobson, Bea-Jane Lin, Cil Davis, Vic Draper, and Phil Flaitz have contributed to this study.

For the use of their experimental facilities, I thank Professors Sumner Davis, Richard Fulrath, Rollie Myers, Joseph Pask, and Milton Pickus.

I thank Gloria Pelatowsky for her consideration in drawing the figures.

I would like to thank the staffs of the Department of Chemistry, University of California and the Lawrence Berkeley Laboratory for their help:

Alloy preparation	Don Krieger, John Holthius
Chemical analysis	G. Shalimoff, V. Tashinian
Electron Microscopy	Ken Gaugler, Rich Lindberg
Glass blowing	Paul Hendrickson
Mechanical Technology	Howard Wood, Glen Baum, Duane Newhart, Weyland Wong
Metallography	Brian Pope, John Jacobsen

This work is supported by the United States Department of Energy under contract number W-7405-Eng-48.

I. INTRODUCTION

A. Objectives and Scope

Work has been done on the zirconium platinum system.[1,2] A discrepancy of four orders of magnitude exists for the activity of zirconium in platinum. The object of this report is to determine the activity of zirconium more accurately, explain the reported discrepancies, and to provide further insight into the effect of electron concentration on alloy thermodynamics.

The zirconium concentration is determined in this project for platinum, platinum-iridium and platinum-silicon alloys.

B. Approach

A variety of methods are available to study the thermodynamic properties of transition metal alloys. The Lewis-acid-base alloys are extraordinarily stable, and this stability is a source of difficulty. Direct vapor pressure methods are a classic technique, but it is difficult to adapt them to study a system where the activity coefficient can be as low as 10^{-10}. Calorimetric methods have been used, but they require special apparatus because stable alloys of this type are unreactive to most reagents. Electromotive force techniques are useful for these alloys. Emf cells are useful for these alloys because they are capable of providing accurate data. However, such cells are limited to 1200°C and in the case of zirconium-platinum alloys, the composition is limited to 25% zirconium. The nitrogen-nitride equilibria technique is chosen

---

1. L. Brewer and P. Wengert, Met. Trans. 4 (1973) 83.
2. P. J. Meschter and W. L. Worrell, Met. Trans. 8A (1977) 503.

because it can be carried out at very high temperatures where equilibrium is more easily obtained.

The experimental approach requires that platinum alloys equilibrate with zirconium nitride. The procedure is to embed a platinum sheet in a matrix of zirconium nitride, heat this sheet in an atmosphere of nitrogen, and analyze the reaction products to determine the zirconium content.

At high temperatures zirconium in the nitride phase diffuses into the platinum alloy phase. The equilibrium condition is given by

$$a_{Zr}^{ZrN} = a_{Zr}^{Zr_xPt_{1-x}} \qquad (1)$$

The activity of zirconium is fixed by the temperature and nitrogen pressure. Equations 2 and 3 illustrate this dependence:

$$a_{Zr} = a_{Zr}^{o} / P_{N_2}^{\frac{1}{2}} \qquad (2)$$

$$a_{Zr}^{o} = e^{\Delta G_f^o ZrN/RT} \qquad (3)$$

Tests are made to ensure that equilibrium is reached, and that the equilibrium is the reaction described by the above equations.

II. THEORETICAL BACKGROUND

The alloys in this study are not commercial products. The interest in these systems is theoretical. Brewer[3] has predicted that metals from the right-hand side of the transition series should interact strongly with metals from the left-hand side. This strong interaction is the subject of this work. To better understand the experimental design a brief description of the Engel-Brewer theory is presented.

The Engel-Brewer theory of transition metal alloys is a chemical approach to bonding in metallic solutions. Brewer uses a three step procedure[4] to analyze and predict the properties of alloys.

The first step is to establish which electronic configuration has the lowest free energy under the given conditions of temperature, pressure and chemical composition. Carbon, for example, takes the s^2p^2 configuration in the gaseous state. The sp^3 configuration is possible but it lies 96 kcal/mole higher in energy.[5] However, in the presence of tetrahedrally coordinated hydrogen, the sp^3 configuration of carbon is lowest in free energy and the required 96 kcal/mole promotion energy is more than regained by the formation of four carbon-hydrogen bonds. The Engel-Brewer theory is successful in rationalizing the behavior of metals because it recognizes that an atom can have different electronic configurations in different environments.

---

3. L. Brewer, Acta Met. 15 (1967) 553.
4. L. Brewer, "Prediction of Transition Metal Phase Diagrams", J. Nucl Mat. 51 (1974) 2.
5. L. Pauling, The Nature of the Chemical Bond, 3rd Ed. Cornell University Press, 1960.

The second step is to determine the number and nature of the bonding interactions. For example, body-centered cubic tungsten with a d^5s electronic configuration has one long-range metallic s bond and five short-range d bonds per atom, while hexagonal close-packed zinc with a $d^{10}sp$ configuration has two s,p long-range metallic bonds and no d bonds. Zinc has ten 3d electrons, but they are internally paired and do not form interatomic bonds.

The third step is to use established physical chemistry theories to predict the properties of materials from their bonding arrangements. The one s electrons in a delocalized orbital make tungsten a thermal and electrical conductor. The five d bonding electrons make tungsten a strongly bound solid with a high melting point, low vapor pressure and small self-diffusion coefficient. Zinc has two bonding s,p electrons. These two long-range s,p electrons are responsible for zinc's high electrical conductivity and high thermal conductivity, as well as a moderate amount of bonding which results in a low melting point and a high vapor pressure at elevated temperatures.

A criticism of Brewer's approach is that it does not deal with the complexities of the electronic interactions. This is an astounding misconception. Brewer's approach is developed specifically to deal with complex systems. By decomposing the properties of metals into periodic factors and calculating the aperiodic factors exactly with optical spectroscopy data, Brewer has clearly organized the trends in the properties of metals so that his use of valence appears elementary.

The result of complex interactions can often vary in a regular manner. This is shown in Fig. 1, a plot of the dissociation energy *vs.* position in the Periodic Table for the first row diatomic molecules. At first the dissociation energy increases with atomic number, then it decreases with increasing atomic number. Even though the electron-electron interactions in these molecules are large, a valence bond approach accounts for this curve and makes accurate predictions possible. Molecules isoelectronic with N_2 have similar dissociation energies as exemplified by $CO(D_0=10.6$ eV) and $NO^+(D^0=10.3$ eV).

The transition metals with both d electrons and s,p electrons prove to be more complex systems. Figure 2 is a plot of various thermal and mechanical properties of the third transition series *vs.* position in the Periodic Table. This plot has the same form as Fig. 1. At first the properties increase with increasing atomic number, reach a peak and decrease with increasing atomic number. The similarity of the two figures suggests that the same valence effects are operating in the transition metals as in s,p valence elements.

The melting curve in Fig. 2 is readilyaccounted for by Brewer's valence bond theory. The results of the three step process is collected in Table 1 for four elements. The details of the calculation of the electronic configuration of the transition metals have been computed.[6] In the first half of the transition series, increasing the number of electrons increases the number of bonds. Tantalum has one more electron

---

6. L. Brewer in Phase Stability in Metals and Alloys,1967, Ed. P. Rudman, J. Stringer and R. L. Jaffee. p. 39.

Figure 1.

Dissociation Energies of Diatomic Molecules *versus* their Group number.

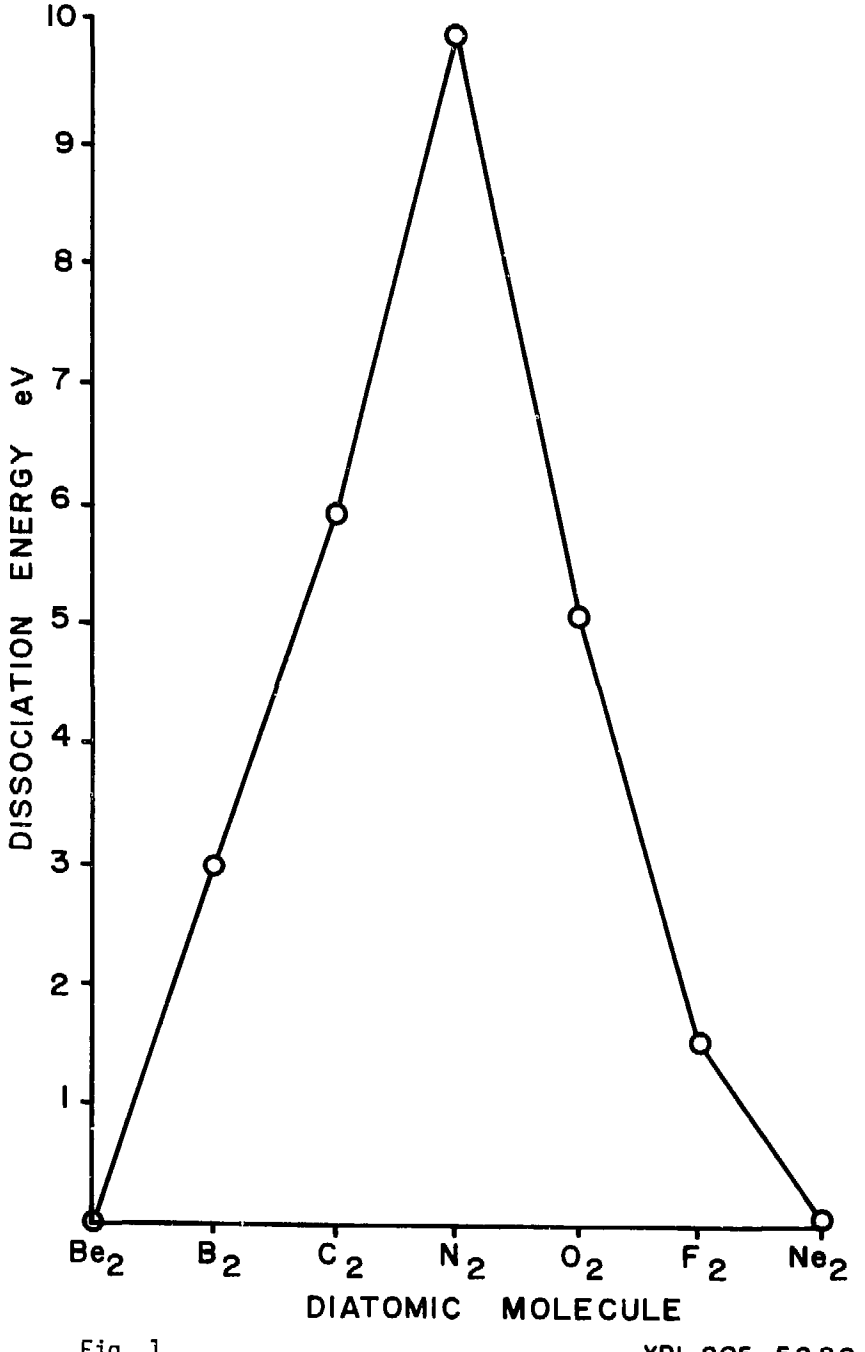

Fig. 1

XBL 805-5222

Figure 2.

Properties of the Third Series Transition Metals.

△ Boiling point ÷ 500 (K)

◇ Cohesive Enthalpy ÷ 20 (kcal/g-atom)

○ Young's Modulus x 2 (kg/cm^2)

□ Bulk Modulus x 2 (kg/cm^2)

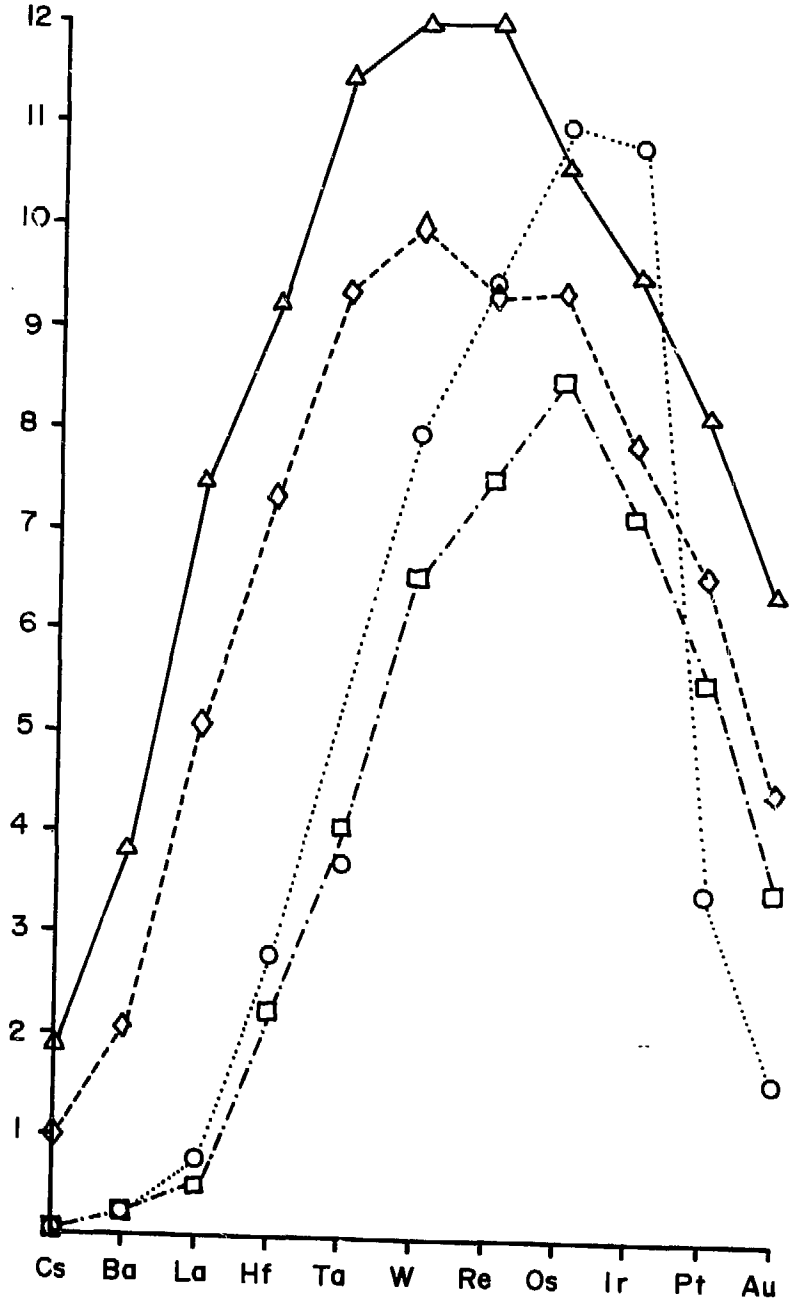

Fig. 2

XBL 805-5223

than hafnium. This extra electron goes into an unoccupied orbital, allowing it to participate in bond formation. Accordingly, tantalum has one more bond than hafnium and as a result it has a higher melting point. In the second half of the third transition series, increasing the number of electrons decreases the number of bonds. Platinum has one more electron than iridium. This extra electron goes into an occupied orbital. The two electrons share the same orbital, spin pair and they are unavailable for bonding. Accordingly, iridium has a higher melting point than platinum.

Table 1 Electronic Configuration and Melting Point

Element	Electron Configuration	Number of Bonding d electrons	Melting Point
Hf	d^3s	3	2222
Ta	d^4s	4	2996
Ir	d^6sp^2	4	2454
Pr	d^7sp^2	3	1769

Brewer's viewpoint of metallic stability suggests a classification of transition metals into three categories according to the orbital occupany of each metal. A metal can have a less than half-filled d shell, a half-filled d shell, or a more than half-filled d shell. Zirconium, d^3s, is a less than half-filled d shell metal. Tungsten, d^5s, is a half-filled d shell metal, and platinum, d^7sp^2, is a more than half-filled d shell metal. The alloying behavior of Zr, W, Pt will be experimentally studied in this report.

The interaction between a less than half-filled d shell metal and a more than half-filled d shell metal is described by Brewer and Wengert as a Lewis-acid-base interaction.[1] Figure 3 shows an example of this interaction. Tantalum with a d^3s electronic configuration has an empty d orbital which can accept electrons. Iridium, d^6sp^2, can utilize the empty d orbital of tantalum by sharing its paired d electrons. As shown in the figure, all the electrons of the product alloy are available for bonding, whereas one of the reactants, iridium has paired non-bonding electrons. This special orbital-electron sharing results in large negative free energies of formation for these Lewis-acid-base alloys. In this report I seek to establish the role of this kind of bonding in the platinum-zirconium system at equal mole fractions of the components.

Figure 3.

The Electronic Configurations of Ta, Ir and $Ta_{.5}Ir_{.5}$.

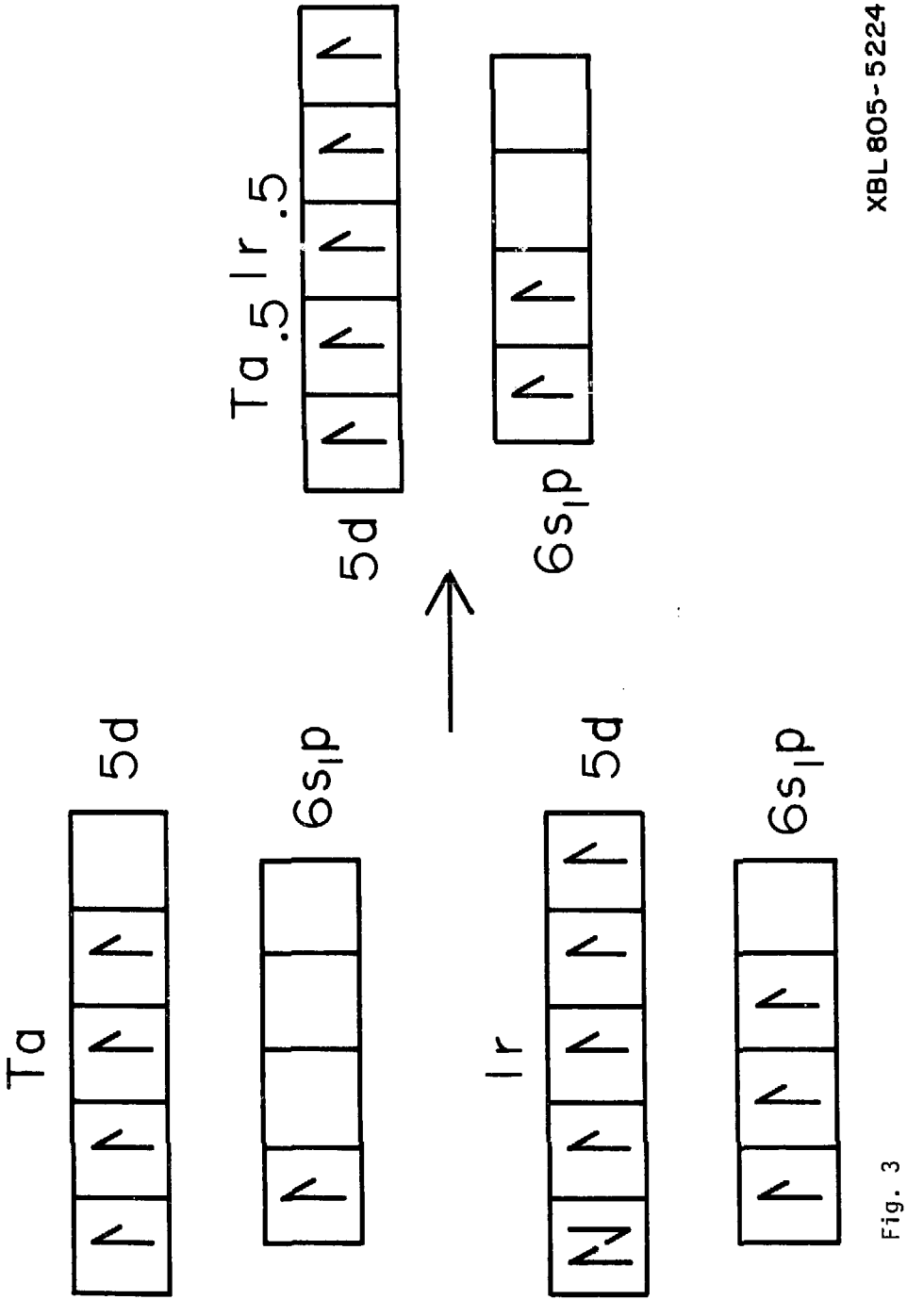

Fig. 3

III. LITERATURE

A literature survey is presented of the principal materials, ZrN and ZrPt, and the principal technique used to establish nitrogen-nitride alloy equilibria. A particularly valuable reference book has been prepared at the Max-Planck-Institut für Metallforschung, Stuttgart.[34]

A. Zirconium Nitride

Only one stable phase exists in the zirconium nitrogen system.[7] ZrN has a NaCl crystal structure with lattice parameter a=4.577 Å. The dependence of the lattice constant on the degree of nonstoichiometry is small and hence an inaccurate method for determing the nonstoichiometry. The melting point of ZrN is 2982°C.

The phase diagram[7] is given in Fig. 4. The homogeneous range extends from ZrN to $Zr_{.6}N_{.4}$. No nitrogen-rich phase has been reported.

The properties of ZrN can vary with its preparation technique because of the large homogeneous range. Only studies with closely controlled stoichiometries were used to formulate the free energy of formation for ZrN. The heat of formation of ZrN is given by Mah[8] for $Zr_{.499}N_{.501}$. Coughlin[9] measured the high-temperature heat capacity and Todd[10] measured the low temperature heat capacity for $Zr_{.501}N_{.499}$. These reports in conjunction with values of the thermodynamic data for Zr and N_2 yield the Gibbs free energy of formation of ZrN in cal/mole:

$$\Delta G_f^o = -87\,085 + 22.21\,T \qquad 1136\text{-}2125K \qquad (4)$$

$$= -90\,740 + 23.865\,T \qquad 2125\text{-}2600K \qquad (5)$$

---

7. L. Toth, Transition Metal Carbides and Nitrides, Academic Press, N.Y., 1971.
8. A. Mah and N. Gilbert, J. Am. Chem. Soc. 78 (1956) 3261.
9. J. Coughlin and E. King, J. Am. Chem. Soc. 72 (1950) 2262.
10. S. Todd, J. Amer. Chem. Soc. 72 (1950) 2914.

Figure 4.

Phase Diagram of the Zirconium-Nitrogen System.

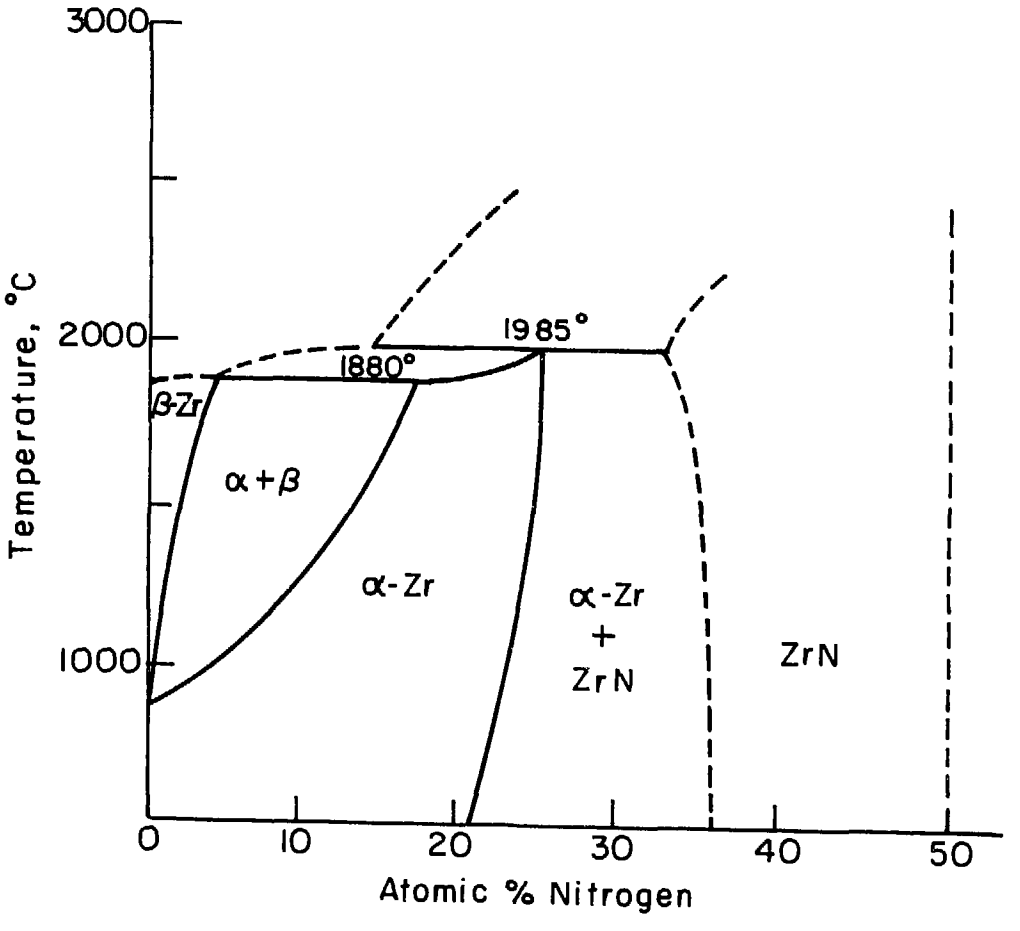

Fig. 4

XBL803-4843

Few reports are available on the thermodynamic properties of non-stoichiometric zirconium nitride. Gal'braikh[11] studied the enthalpy of formation of ZrN_x with the result

$$\Delta H^o_{298} = -48.3 - 40.5x \text{ kcals/mole} \quad .78 \leq x \leq 1 \tag{6}$$

For the stoichiometric composition his result is 10% more negative than that of Mah. Inaccurate thermodynamic data for the nonstoichiometric compositions indicate that preliminary experiments on nitrogen nitride equilibria should be carried out with the stoichiometry compositions.

Desmaison[12] measured the diffusion of nitrogen in $ZrN_{.93}$ and reports

$$D_N = 4\times10^{-6}\, e^{-36\,600/RT}\ cm^2/sec \tag{7}$$

for the temperature range 1000-1200°C. Extraplation to 2000°C and calculation of the diffusion length, $\bar{x}$, with the approximation $\bar{x}=2\sqrt{Dt}$ yields $\bar{x}$=83 microns/4 hours. This is more than twice the largest particle size.

B. Zirconium Platinum

Phases of the zirconium platinum system are given in Table 2. Figure 5 is the preferred phase diagram[13] augmented by the work of Meschter [14], Dwight[16], and Panda[18].

Thermodynamic studies on the zirconium platinum system are numerous primarily for compositions of 25 atomic per cent zirconium or less. Stowe *(see ref. 1)* reacts a mixture of ZrO_2 and platinum in a hydrogen atmosphere at 1420K. The reaction product is determined to be $ZrPt_3$ and the free enthalpy of formation is $ZrPt_3 \leq -81.8$ kcal/mole.

---

11. E. Gal'braikh, *et al.* Poroshkovaya Metallurgiya 93 (1970) 62.
12. J. Desmaison and W. Smeltzer, J. Electrochem. Soc. 122 (1975) 354.
13. E. Kendall, C. Hays and R. Swift, Trans. Met. Soc. 221 (1961) 445.
14. P. Meschter, Ph.D. Thesis, University of Pennsylvania. 1974.

Figure 5.

Phase Diagram of the Zirconium-Platinum System.

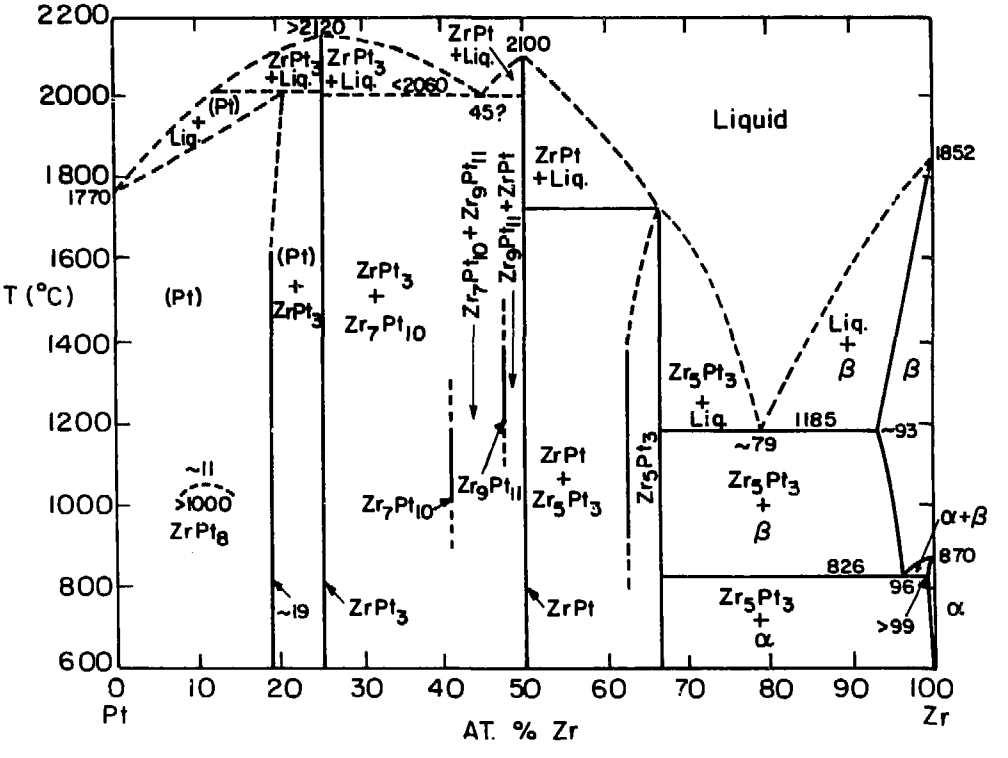

Fig. 5

XBL805-5212

Table 2. Phases in the System Zirconium-Platinum and Lattice Parameters (Å)

Phase	Structure	Lattice Parameter(Å) a	b	c	Reference
Zr	W	3.61			15
Zr	Mg	3.23		5.15	15
Zr_5Pt_3	Mn_5Si_3	8.2		5.4	16
ZrPt (*high temp*)	CsCl	3.31			17
Zr_9Pt_{11}	tetragonal	10.3		6.89	14
Zr_7Pt_{10}	tetragonal	6.78		13.03	14
$ZrPt_3$	$TiNi_3$	5.63		9.22	19
Pt	Cu	3.92			15
Zr_6Pt_3O	$TiNi_2$	12.49			20

---

15. A. Maldonado and K. Schubert, Z. Metallkde. 55 (1964) 619.

16. A. Dwight, Trans. Met. Soc. AIME 215 (1959) 283.

17. A. Dwight, R. Conner and J. Downey, Acta Cryst. 18 (1965) 835.

18. S. Panda and S. Bhan, J. Less. Comm. Met. 34 (1974) 344.

19. A. Raman and K. Schubert, Z. Metallkde. 58 (1967) 558.

20. M. Nevitt, J. Downey and R. Morris, Trans. Met. Soc. AIME 218 (1960) 1019.

Carbonara and Blue[21] use a mass spectrometer to measure the vapor pressure of Pt, ZrO and Be emanating from a knudsen cell containing $ZrPt_3$ and BeO. They report the free energy of formation of $ZrPt_3$=-82.1 kcal/mole.

Srikrshnan and Ficalora[22] measure the enthalpies of formation of $ZrPt_3$ by fluorine bomb calorimetry. The enthalpy of formation of $ZrPt_3$ is determined to be -122 kcal/mole.

Brewer and Wengert[5] equilibrate ZrC, graphite and platinum at 1850K. The reaction product contains $ZrPt_3$. The free energy of formation is reported as -30 kcal/gatom and $a_{Zr}^{ZrPt_3}=5\times10^{-6}$ at 1800K.

Meschter and Worrell[23] utilized electrochemical cells of the type

$$NbO_2,Nb_2O_{4.8} \mid ThO_2(Y_2O_3) \mid \underline{Zr}(Pt),ZrO_2 \qquad (8)$$

to determine the activity of zirconium in platinum. They compute $a_{Zr}=6.5\times10^{-16}$ at 23 at pct Zr and the free energy of formation is -91.7kcal/mole.

Finally Schaller[24] determines the activity of zirconium in platinum up to 25 at% zirconium. Schaller uses a procedure similar to that of Stowe, but with much better control of the gas composition. Results are similar to those of Meschter.

Table 3 summarizes the results of the different investigations.

Table 3 Comparison of ΔG_f^o $ZrPt_3$

Investigator	T(K)	$-\Delta G_f^o$ $ZrPt_3$ kcal/mole
Stowe	1273	≥81.3
Carbonara	2200	82.1
Wengert	1800	120
Meschter	1300	91.7
Schaller	1273	89.2

21. R. Carbonara and G. Blue, High Temp.Sci. 3 (1971) 225.
22. V. Srikrishnan and P. Ficalora, Met. Trans. 5 (1974) 1471.
23. P. Meschter and W. Worrell, Met. Trans. 8A (1977) 503.
24. H. Schaller, Ber.Bunsenges.physik.Chem. 80 (1976) 999.

Wengert reports the activity of Zr in $ZrPt_3$ as 5×10^{-6}. Extrapolation of Meschter's results to Wengert's reaction temperature produces a zirconium activity of 2.4×10^{-9}, a difference of three orders of magnitude. Useful bonding models are possible only if the properties of these systems are better understood. This study will resolve the differences between these two results.

C. Alloy Nitride Equilibria

Two types of experiments have been carried with alloy nitride equilibria. In the first type of experiment the alloy composition is fixed and the nitrogen pressure is varied.[25,26,27] Pehlke and Evans[25] studied zirconium iron alloys with this technique. The reaction,

$$Zr_{Fe} + N_{Fe} \rightarrow ZrN, \qquad (9)$$

takes place in a Sieverts apparatus. Alloys of fixed composition are equilibrated with small increments of nitrogen and the pressure of the system is monitored. After the critical concentration of nitrogen is reached, additions of nitrogen do not raise the pressure in the system because they are converted to zirconium nitride. When the results of these experiments are used to calculate the activity of the solute metal in the solvent metal, the activites vary erratically. The problem might arise from poor characterization of the precipitated nitride because it is merely X-ray analyzed. Since these transition metal nitrides have large homogeneous ranges, another method was sought that would give better control over the nitride phase composition.

---

25. D. Evans and R. Pehlke, Trans. Met. Soc. 230 (1964) 1651.
26. N. El Tayeb and N. Parlee, Trans. Met. Soc 227 (1963) 929.
27. F. Baehren and D. Vollath, Planseeb für Pulvermet. 17 (1969) 180.

In the second type of alloy nitride equilibrium experiment, the nitrogen pressure is fixed and the alloy composition adjusts.[28-30] Brewer and Krikorian[28] obtain heats of formation for groups 4 and 5 metal silicides by equilibrating the alloys in nitrogen and determining the reaction products by X-ray analysis. The agreement of these calculations with the calorimetric determiantion of Robins and Jenkins is good.[31] The advantage of this technique is that one has excellent control of the nitride phase. Since the thermodynamic data for the alloy will be no better than that of the nitride phase, the nitride stoichiometry must be fixed and accurately known. In this study, the second technique is used.

---

28. L. Brewer and O. Krikorian, J. Electro. Chem. Soc. 103 (1956) 38.
29. L. Brewer and H. Haraldsen, J. Electrochem. Soc. 102 (1955) 399.
30. E. Turkdogan and P. Grieveson, Trans. Met. Soc. AIME 227 (1963) 1143.
31. D. Robins and I, Jenkins, Acta. Met. 3 (1955) 598.

IV. APPARATUS and PROCEDURES

A description of the experimental apparatus, the procedures used to prepare and react the specimens, and the methods used to analyze the reaction products is presented.

A. Description of the Apparatus

The experimental apparatus is shown in Fig. 6. Temperatures to 2300°C are obtained with a graphite resistor King furnace [3]. The temperatures are measured with an optical pyrometer [1] sighting through a quartz window [2]. The furnace is evacuated with a mechanical pump [5]. Argon [6] or nitrogen [7] pass through an absorbant[31] [9] to remove oxygen and water. The compound pressure/vacuum gauge [8] indicates the pressure in the system. The gas lines in the section above the apparatus are made of stainless steel which is degreased, acid cleaned and rinsed in distilled water. The valves are stainless steel Nupro bellow valves. The pressure measurement apparatus [10-13] is all glass. A Kovar to Pyrex seal joins the metal lines to the glass tubing. A dry-ice acetone trap [10] protects the McLeod gauge [11] and mercury U-tube manometer [12] from condensible vapors. A mechanical pump [14] evacuates the gauges through a liquid nitrogen trap [13]. The valves on the pressure measurement section are glass high-vacuum stopcocks.

---

31. Oxisorb, manufactured by MG Scientific Gases, Somerville, N. J.

Figure 6.

Nitrogen-Nitride-Alloy Equilibrium Apparatus.

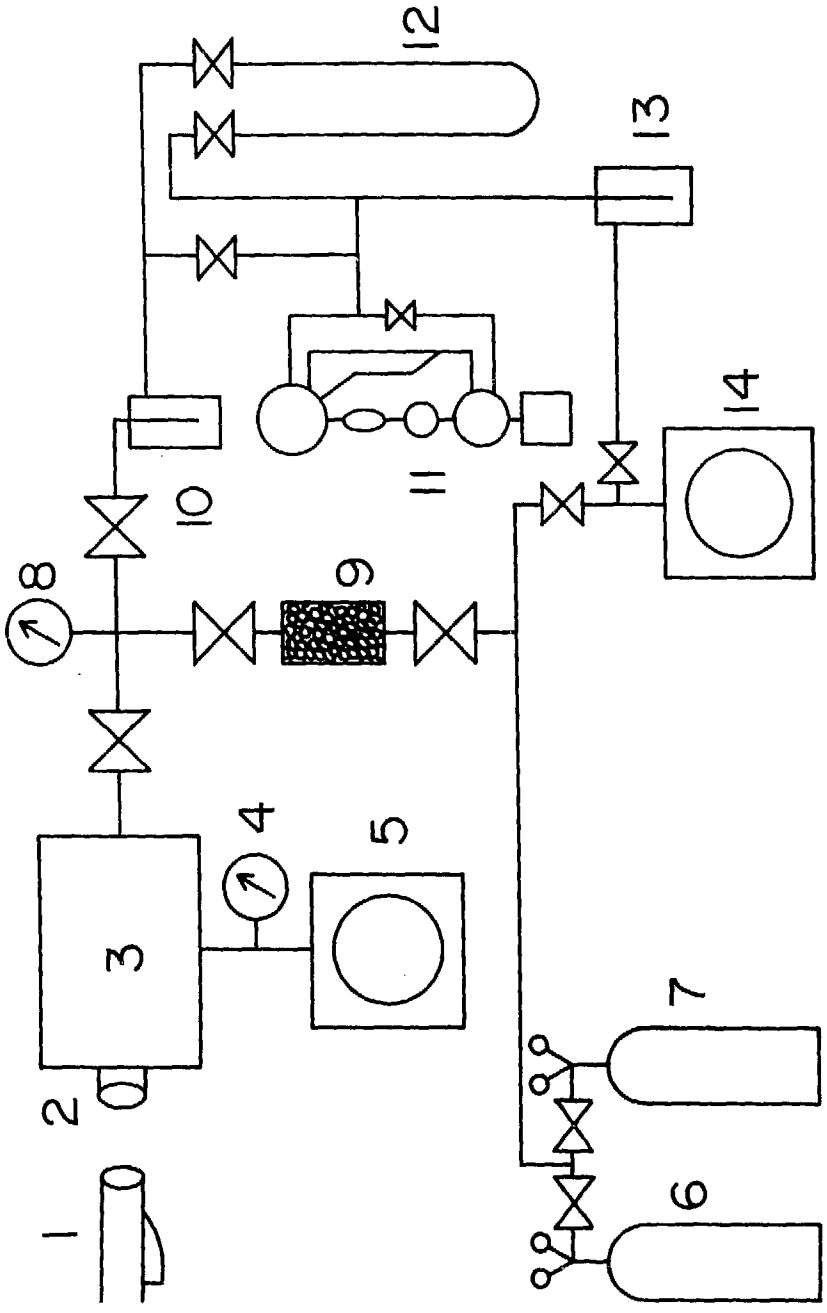

XBL805-5221

Fig. 6

B. Pellet Fabrication

The following procedure is used to make the reaction pellets. Naphthalene(8 vol%) is dissolved in anhydrous ethyl ether and mixed into -325 mesh powders of zirconium nitride. The ether is volatilized under reduced pressure leaving a coating of naphthalene on the nitride particles. Approximately 1.5 gm of nitride is placed in a 0.5" ID steel die; the powder is compacted lightly, an alloy disc 0.25" OD is laid and centered on top of the nitride compact, 1.5 gm of nitride is added again on top of the alloy, and this mixture is pressed at 10 tons/in^2. (At this pressure the nitride compact is compressed to 63% of its theoretical density.) The finished specimen is a nitride pellet, 0.5" in diameter, 1/3" long which contains a noble metal alloy. A 3/64" black body is drilled into a face of the pellet to a depth of 0.25". The specimen is placed in a 120^{o}C oven and left overnight to bake out the naphthalene.

C. Alloy Fabrication

Alloys are made from the materials listed in Table 4.

Table 4. Forms of Pure Metals

Metal	Form
Zirconium	≤1/8" to +20 mesh
Platinum	.001" foil,.002"sheet,.01" sheet
Iridium	.02" sheet
Tungsten	.001" foil
Molybdenum	.001" foil
Silicon	≤1/8" to +20 mesh

Weighed portions of acid-cleaned metals are arc-melted with a tungsten electrode on a water cooled copper hearth. A gettered argon atmosphere is used to limit evaporation losses. Weight loss is typically .03%. The

alloy buttons are flipped and remelted three times. The pellets are annealed for four hours 200°C below their melting point. The alloy buttons are cut into thin specimens on a low speed diamond wheel. Tin snips are used to shape the specimens into a disc. The alloys are cleaned in acid, rinsed and dried. Prior to embedding the alloy in nitride, they are weighed, the thickness is measured, and they are cleaned ultrasonically in a soap solution, rinsed and dried.

D. Equilibration Schedule

A typical equilibration run proceeds as follows. The surface of the pellets are lightly ground in order to remove contamination picked up from the steel die walls. Identification marks are scratched into the pellet surface and each pellet is weighed. The pellets are loaded into a tungsten-lined graphite tube whose quartz window is cleaned with Kodak lens cleaner, the furnace is evacuated to 20 microns, and a rate of rise measurement performed. The furnace is brought up to 1000°C and left under vacuum for 15 min in order to remove some of the adsorbed vapor. The furnace is isolated from the vacuum pump, nitrogen gas is admitted, and the temperature is increased at a rate of 70°C/min. After reaching temperature, the temperature and pressure measurements are made every hour. The run is terminated by quickly turning down the power, the sample cools from 2000°C to 1000°C in 3 mins. Pellets fired at 2000°C for 4 hrs lose 1-4 wt%.

E. Chemical Analysis

Gravimetric methods are used to determine the alloy compositions.

The alloy must be cleanly separated from the nitride in order to obtain accurate results. It is important to eliminate nitride on the

surface because it will lead to results too high in zirconium. Many acid combinations were tested in order to determine a combination that would dissolve nitride, but not the alloy. The best solution determined consists of 11M H_2SO_4, .7M HNO_3 and .8M $HClO_4$. This acid readily attacked the nitride without producing an alloy weight loss. Acid cleaned alloys sometimes had light gray or black deposits on the surface. Figure 7 is a micro-photograph of a discolored area. Apparently at reaction temperatures the liquid alloy creeps into the nitride matrix. When the nitride is etched away a rough surface is left which interacts with light to produce off-tones.

Zirconium-platinum alloys are hard to dissolve. Zirconium is resistant to most acids with the exception of HF, and platinum is resistant to most acids with the exception of aqua regia. When these materials are alloyed and their activities lowered by five orders of magnitude, the dissolution is slow even in strong acids. The alloys are treated with a 25 ml solution composed of 3M H_2SO_4, 1.5M $HClO_4$ and 1.4M HNO_3. Then 10 ml of aqua regia and 4 ml 48% HF are added. The mixture is stirred with a Teflon rod, left overnight in a vitreous carbon crucible and then placed on a hot plate and heated for three hours. This treatment dissolves all the alloys. The crucible is slightly eroded, but the carbon particles in the precipitate are converted to CO_2 in the subsequent ignition. The temperature is increased and the solution fumed to half its volume to remove HF. The walls of the beaker are washed down with distilled water and the solution is evaporated to complete dryness. This removes traces of fluoride which would complex zirconium.

Figure 7 .

Alloy Surface (magnification 165x, 1 inch = 150 microns).

Fig. 7

XBB805 6420

The zirconium content of the alloys is determined by organic reagents. Mandelic acid (hydroxy-phenyl acetic acid) is used to analyze all zirconium alloys. The procedure of Norwitz[31] for the determination of zirconium by mandelic acid gives excellent results. The only interferring metals are Ti, Sb, Bi and Sn.[32]

The dry alloy salt is redissolved in 20 ml of hot 3.4M HCl. The contents of the glassy carbon crucible are transferred into a beaker; three washes of the crucible using 1.5M HCl are used, 30 ml of 1M mandelic acid added to the solution. A 5.5 cm diameter Whatman number 42 paper is cut into small pieces and placed in the solution as filter pulp in order to increase the retention of fine particles. The beaker walls are washed down with distilled water, the top of the beaker is covered with a watch glass and the beaker is placed in an 80°C oven to digest overnight.

The filtration is done at room temperature through a number 42 Whatman ashless filter paper, 11 cm in diameter. The precipitate is washed with a .3M mandelic acid, 1M HCl wash solution. The filter paper is folded into a porcelain crucible and this is heated over a bunsen burner with limited access to air to turn the carbonaceous material to coke. The crucible is cooled to room temperature and placed in an electric furnace. The sample is fired at 950°C overnight, allowed to cool in a dessicator and the zirconium weighed in the form of ZrO_2. Using

---

31. George Norwitz, Anal.Chim.Acta 35 (1966) 491.
32. R. Young in Chemical Analysis in Extractive Metallurgy, Barnes and Noble, 1971. 384.

this procedure, 41.7 mg of zirconium is recovered from a standard solution containing 42.5 mg.

The filtrate from the mandelic acid determination of zirconium is analyzed for platinum. The method described by Walsh and Hausman[33] for the sulfide precipitation of platinum gives results accurate to 1 mg. The mandelic acid filtrate is boiled and then removed from the hot plate. Hydrogen sulfide is passed through the solution at a rate of one bubble/sec. The precipitation continues until the solution has cooled to room temperature. The gas bubbler is removed and rinsed out and the solution is boiled to coagulate the precipitate. The solution is cooled to room temperature, filtered through Whatman number 42 paper; the precipitate is washed with distilled water and folded into a porcelain crucible. The crucible is heated over a bunsen burner with limited access to air, then placed in an electric furnace and heated at 950°C overnight. The residue is weighed as Pt.

To validate the analytical procedure, a test alloy was prepared. An 8 gm sample of $Zr_{.59}Pt_{.41}$ is prepared from zirconium chunks and platinum foil. The mixture is arc-melted, and the weight loss due to evaporation is .03%, small enough so that the composition of the alloy is taken as that of the weighed mixture. The alloy button is then homogenized at 1600°C for 4 hrs. The sample is sliced into specimens, one of which is mounted in bakelite and polished to 1 micron. The specimen is etched in hydrofluoric acid to expose the microstructure. The test alloy, $Zr_{.59}Pt_{.41}$,

---

33. Thomas J. Walsh and Eugene A. Hausman in Treatise on Analytical Chemistry, Part II, Vol. 8, I. M. Kolthoff, Ed. 1963. p. 379.

corresponds to an equal mixture of the phases ZrPt and Zr_5Pt_3. The alloy microscopically examined consists of two phases of roughly equal volume. No large inhomogeneities are seen. A 92.1 mg sample of this alloy chemically analyzed contains 37.2 mg zirconium and 55.3 mg platinum. The computed composition is $Zr_{.59\pm.02}Pt_{.41\pm.02}$. The close match between the analyzed and actual composition and the small weight gain (approximately .5%) of the alloy after chemical analysis confirms the method used.

F. Nitride Non-Stoichiometry Analysis

Accurate control and analysis of the nitride stoichiometry is crucial because their thermodynamic properties vary with the degree of nonstoichiometry. The following procedure is used to measure the nitrogen content of the alloys. A 0.3 gm nitride specimen is cut from the reacted pellets with a hack saw. Any surface imperfections are removed by grinding on SiC paper. The nitride is weighed and fired at 950°C overnight to convert the nitride to zirconium dioxide. The weight gain of the sample allows calculation of the orginal nitrogen content. A standarization is performed with aluminum nitride. It is a covalently bonded solid and therefore a stoichiometric compound. The determined composition is $Al_{.49\pm.003}N_{.51\pm.003}$. For the determination of ZrN 1 at% is subtracted from the nitrogen content and added to the metal content. All analyses on ZrN equilibrated in 1 atm of nitrogen or higher yield the stoichiometric composition.

G. X-ray Analyses

A Picker X-ray Diffractometer is used for X-ray analysis. The nitride phase always has the same spectrum. The alloy phases are a

problem. I am not able to obtain well-defined X-ray spectra of the product alloys. All reported phase analyses are based on a determination of the composition and temperature and use of the phase diagram to identify the product phases.

H. Interstitial Elements Analyses

The interstitial elements hydrogen, carbon, nitrogen and oxygen are soluble in zirconium and can affect its properties. At 1500°C 2 at% C, 6 at% N and 10 at% O can dissolve in zirconium.[34] At 1500°C platinum can dissolve 0.3% C, 0.01% O and almost no N.[34] I have found no data on interstitial solubility in platinum-zirconium alloys, but Hoerz, *et al.*[35] have studied the solubility of nitrogen in niobium-rhenium alloys. They found that a 40 at% rhenium alloy had a nitrogen solubility 1.5 orders of magnitude smaller than that of pure niobium. In the zirconium-platinum system I expect platinum to inhibit the solubility of the interstitials in zirconium just as rhenium does in niobium. All of my results will be for alloys equilibrated in 500-900 torr of nitrogen.

Three methods are used to analyze for interstitial elements: optical metallography, scanning electron metallography and Auger spectroscopy. At the high temperatures at which the nitrogen equilibria are carried out, C, N and O can dissolve in the alloys when the alloys are cooled; if large amounts of C, N and O are present, ZrC, ZrO_2 or ZrN would precipitate out of solution. To determine if these precipitates formed, alloy specimens

---

34. E. Fromm and E. Gebhardt, Gase und Kohlenstoff in Metallen. Springer-Verlag, Berlin. 1976.

35. G. Hoerz and R. Ziegeldorf, Z. fuer Metallkunde. 67 (1976) 661.

were sectioned, mounted in bakelite ground on SiC paper, and polished to 1 micron with diamond paste. The polished surface is then examined under a microscope for defects. Figure 8 shows a typical specimen viewed through an electron microscope. It is a two phase zirconium-platinum alloy and no irregularly shaped or tinted third phase is seen. In niobium alloy 0.01 weight percent nitrogen is readily seen at 100x magnification.[36]

The scanning electron microscope with its tremendous depth of field allows sharp pictures to be taken inside pores. Figure 9 shows an electron micrograph of a porous specimen. The surface has many voids. A third-phase might have filled these voids in the reaction environment. Later during the processing of the specimen the third phase could have been lost. During polishing a third phase could have been lost. When polishing a two-phase region, one phase of which is ductile like a metal, and the other phase is brittle like a ceramic, the ceramic phase is often ripped out. Figure10 examines the inside of one of these voids. The surfaces are smooth and the many nooks and crannies would have held a third-phase in place.

For the Auger analysis a sample alloy is prepared for interstitial analysis as follows: a 0.002" thick, 0.25" OD disk of platinum is embedded in ZrN and fired at 1815^{o}C for two hours at 875.5 torr of nitrogen. The activity of zirconium under these conditions is 4.5×10^{-5} and the diffusion limited reaction product will be about $Zr_{0.35}Pt_{0.65}$. A slow speed diamond wheel is used to gently cut the pellet in half. The cross-section containing

---

36. E. deLamotte, Y. Huang and C. Altstetter, Trans.Met.Soc AIME 239 (1967) 1675.

Figure 8.

Alloy Nitride Cross-Section (magnification 160x, 1" = 150 microns)
Left-hand side Layer: Bakelite mounting material
Middle Layer: Zirconium-platinum Alloy
Right-hand side Layer: Zirconium-nitride

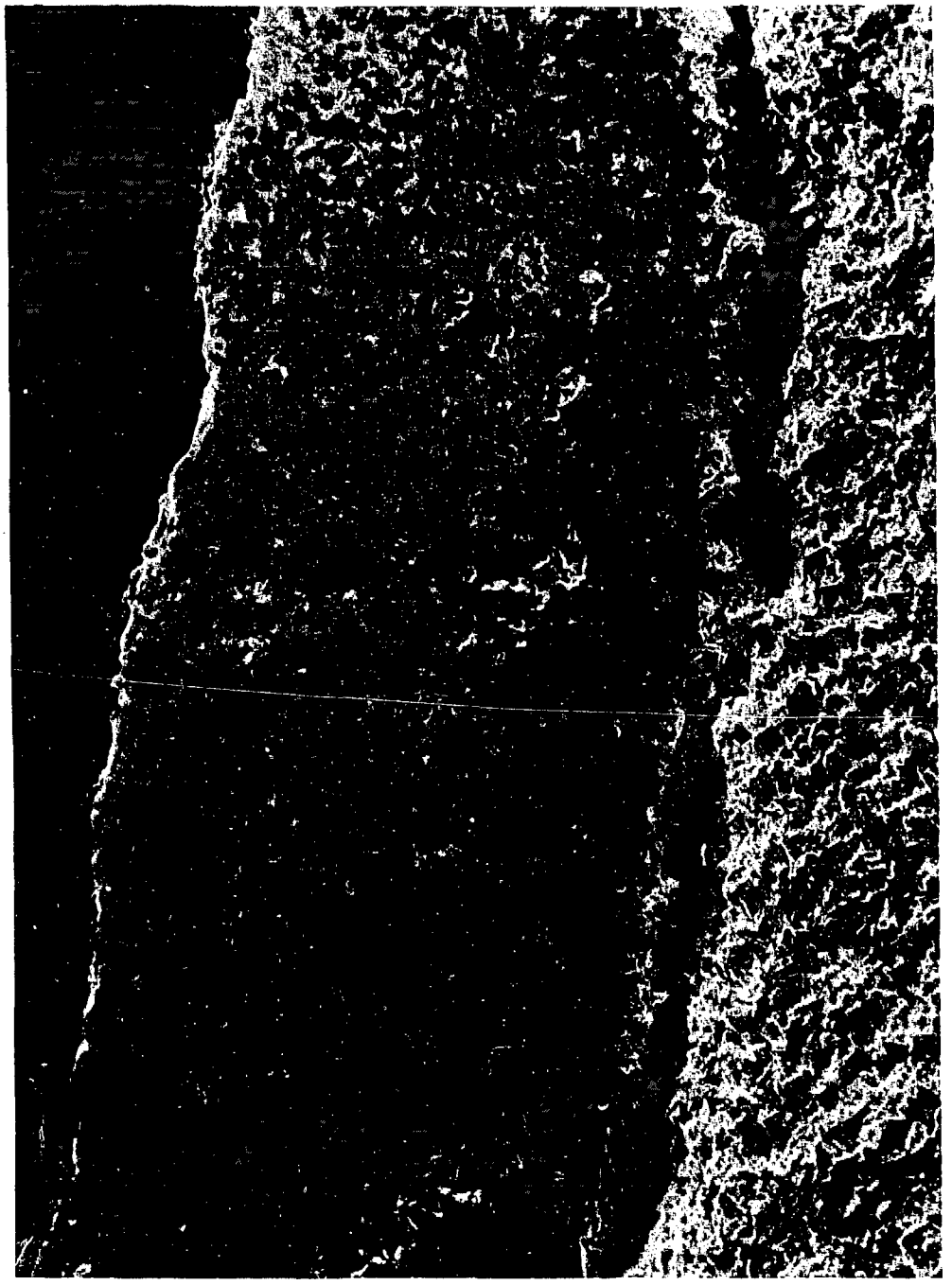

Fig. 8

XBB805 6418

Figure 9.

Surface of Alloy (magnification 1700x, 1 inch = 15 microns).

Fig. 9

XBB805 6416

Figure 10.

View inside a Void (magnification 8500x, 1 inch = 3 microns).

Fig. 10

XBB805 6417

the platinum-zirconium nitride interace is carefully ground on SiC paper and polished to 1 micron with diamond paste. The sample is ultrasonically cleaned in a soap solution, rinsed and baked out in an oven overnight.

A qualitative elemental analysis of the specimen is performed with an Auger spectrometer (Physical Electronics Industries). In the spectrometer 5 keV electrons bombard the sample, knocking core electrons out of the atoms. In the case of oxygen an electron is ejected from the K level leaving a vacancy. An L electron falls into the lower energy K shell. The energy difference is emitted during the L to K shell electron transition. The second way energy is emitted is by the ejection of the second electron in the L shell. This is the Auger effect, and the energy of the emitted electron is characteristic of the emitting element. Table 5 gives the positions of the most intense peaks for the elements of interest.[37]

Table 5. Auger Peak Positions

Element	Peak Position (eV)
Zr	21, 147
Pt	64, 43
N	379, 360
O	503, 483
C	272
Ca	291

The escape depth of the ejected electrons is only five to ten atomic layers because electrons are charged particles and interact strongly with atoms.

---

37. L. E. Davis, *et al.* Handbook of Auger Electron Spectroscopy. Physical Electronics Industries, Eden Prairie, Minn. 1976.

Thus Auger analysis is a surface technique. Absorbed species on the surface of the sample must be eliminated to obtain meaningful spectra. After the sample is introduced into the spectrometer, it is pumped down to 1.6×10^{-9} torr. A spectrum is taken of the unclean surface, then the surface is etched by a 3keV argon ion beam. Based on comparison with other materials, I expect 2000 Å to be etched away.

Auger peaks are superimposed on a large background, therefore spectra are plotted as dN/dE vs. E, rather than N vs. E. The Auger spectrum of the unetched alloy has a dominant peak at the 503 eV oxygen position. The carbon (272 eV) and zirconium (21 eV) peaks are equally strong. Nitrogen has a distinct peak, while platinum gives a weak signal. Calcium is observed; it is probably a residue of the soap solution. The alloy is then etched for 5 min to a depth of approximately 2000 Å. The new spectrum, Figure11, has an intense zirconium peak and the platinum 64 eV peak is distinct. The carbon, nitrogen and oxygen peaks are still present. The peak height of the derivative of the emitted electron intensity depends on so many parameters that quantitative results cannot be obtained. Table 6 gives a rough measure of the relative sensitivities of the elements.[37] The interstitial elements are in the alloy in significant concentrations. Ten points on the alloy are analyzed with similar results. I could not detect any regions of extra high carbon, nitrogen or oxygen content. This provides evidence in addition to the metallographic examination that no precipitates of ZrC, ZrN or ZrO_2 formed in the alloy upon cooling.

Figure 11.

Auger Spectrum of an Etched Alloy.

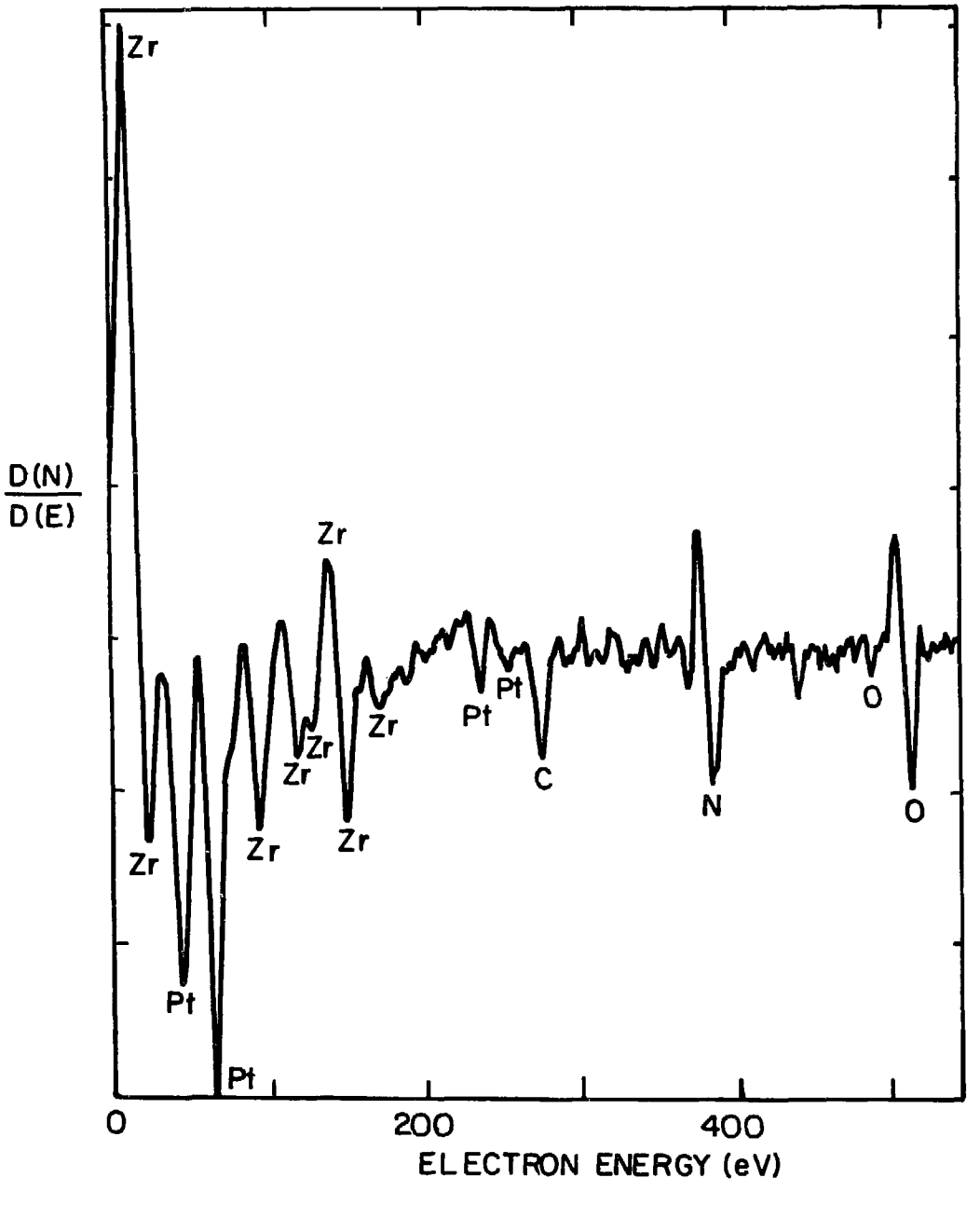

Fig. 11

XBL 805-5193

The lack of sources of oxygen in the experiments suggests that its impurity content should be low. Oxygen is available in the form of water and oxygen gas. The first will be eliminated during the initial heating and degassing of the furnace under vacuum. Any source of oxygen at the equilibration temperatures should react with the nitride before reaching the alloy, which is buried in zirconium nitride. The oxygen content of the furnace is small; tantalum that is heated in the furnace comes out with a bright surface and not a dull oxide coating.

The carbon in the alloy can come from four sources. The first is the carbon impurity in zirconium nitride, reported to be 0.02 at%. The second is surface contamination by hydrocarbons on the platinum. The platinum is cleaned in nitric acid and handled with tweezers so this should not be significant. A third source is from reaction products of nitrogen with the graphite tube at 2000°C, but the hydrogen cyanide formed would react with the hot nitride surface to form zirconium carbonitrides before reaching the alloy.

Table 6. Relative Sensitivities to Auger Analysis

Element	Relative Sensitivity
Zr	0.15
Pt	0.05
O	0.4
C	0.23
N	0.25

Acetylene may be formed in the King furnace. However, the metal is surrounded by 3/16" zirconium nitride; any gas molecules would react with the nitride surface forming ternary zirconium-nitrogen-carbon phase before reaching the alloy. The fourth source is the naphthalene used as

a binder for the nitride. The pellets are baked out overnight at 120°C; after 1/2 hr in the oven the smell of naphthalene is not present. Strong support that the carbon comes from impurity in the nitride phase is found in the Auger spectrum of zirconium nitride. The peak height of carbon in the nitride where the concentration is known is the same as in the alloy. The comparison of the spectra suggests that the carbon content could be as low as 0.02 at% and the nitrogen and oxygen as low as 0.03 and 0.015 at%, respectively.

In summary, carbon, nitrogen and oxygen are present in the alloys, but not in such large quantities as to form precipitates. An estimate of the interstitial impurity content is 0.1 at% or less. At this low concentration 99% of the bonding will be due to metal-metal interactions; the interstitial content does not seriously affect my results.

I. X-ray Fluorescence

An X-ray fluorescence technique is evaluated for use in determining the alloy composition. A sample of $Zr_{.25}Pt_{.75}$ and $Zr_{.41}Pt_{.59}$ is prepared and a 30 keV electron beam is directed to a spot on its surface. Table 8 presents the relative intensities of the emitted X-rays from the zirconium K line (15.8 keV) and the platinum L line (9.4 keV).

Table 8. X-Ray Fluorescence Intensities from Zirconium-Platinum Alloys

	X-ray intensity	
Phase	9.4 keV	15.8 keV
$Zr_{.25}Pt_{.75}$	38 614	7 533
$Zr_{.41}Pt_{.59}$	6 144	15 916

The X-ray fluorescence technique is rejected as a method of analyzing alloy compositions, because of the large corrections that must be made for atomic number, absorption and secondary fluorescence effects.

V. SOURCES OF ERROR

A. Ternary Phase Formation

The formation of a ternary zirconium-platinum nitrogen phase is a major potential stumbling block in this study. For the nitrogen-nitride alloy equilibria to work, the zirconium activity must be fixed by a phase of known thermodynamic properties. A large mass of zirconium nitride is used as a reservoir of constant zirconium activity. If another phase forms at the alloy nitride interface, the zirconium activity could change by a significant amount.

Holleck and Thümmler[37] claim to have prepared Zr_4Pt_2N and twenty-two other ternary transition metal nitrides. In this short communication only a few experimental details are given. Fine powders are cold pressed, the pellets are sealed in quartz ampoules, heated for an unstated time, temperature and pressure. The reaction products are analyzed by X-ray diffraction only. Fortunately, I cannot reproduce the results and a ternary platinum nitride has not been observed.

It appears that Holleck and Thümmher misinterpreted the role of zirconium nitride dissociation on their experimental design. First of all, it is standard procedure to evacuate quartz ampoules and backfill them with argon, and second, the accurate measurement of the gas pressure in a sealed ampoule at reaction temperature is

---

37. H. Holleck and F. Thümmler, Mh. Chem. 98 (1967) 133-4.

difficult to obtain. This suggests that they did not control the nitrogen pressure in their experiments. At 1500°C, the pressure of nitrogen in equilibrium with zirconium metal and zirconium nitride is 10^{-8} atm. At this low pressure the rate of zirconium nitride decomposition is small. However in the presence of platinum, intermetallic compounds can form and greatly reduce the activity of zirconium. The pressure of nitrogen in equilibrium with ZrN and $ZrPt_3$ is 100 atm. If Holleck and Thümmler heated the samples at reduced pressure, intermetallic compounds should form.

I believe that their reaction product is the alloy Zr_6Pt_3O. They report that Zr_4Pt_2N has a Ti_2Ni structure with lattice parameter 12.43 Å. Nevitt *et al.*[38] report an oxygen-stabilized zirconium platinum phase, Zr_6Pt_3O, with a structure of Ti_2Ni and a matching lattice constant of 12.49 Å for well-characterized samples. Presumably, Holleck and Thümmler heated their samples in purified argon and under this condition the starting nitride will dissociate to form nitrogen gas and metal. The zirconium will react with the platinum to form an alloy which will pick up oxygen from the quartz sample container.

---

38. M. V. Nevitt, J. W. Downey and R. A. Morris, Trans. AIME 218 (1960) 1019.

Although the report of Holleck and Thümmer is dubious, it is possible that other ternary Zr-Pt-N exist. Ternary A-B-O phases for similar systems are known.[34] At the low zirconium activity, 10^{-3} to 10^{-5}, of these experiments a Zr-Pt-N phase would be unstable and disproportionate.

It is necessary to confirm that a Zr-Pt-N phase did not form and consequently invalidate the results; the platinum content of the nitride phase is determined. No platinum is detected at a sensitivity of 0.2 at%. An Auger spectrum is taken of the nitride 20 microns from the alloy-nitride interface.

The platinum 64 eV peak is missing, suggesting that the platinum content of the nitride phase is low. This is evidence that the phase in contact with the alloy is the thermodynamically well characterized ZrN phase.

B. Temperature

Temperatures are measured with a Leeds and Northrup optical pyrometer, serial number 709371. This pyrometer is calibrated against another pyrometer which has been calibrated by the National Bureau of Standards using the 1948 temperature scale. A list follows which compares these calibrations.

Table 7 Pyrometer Calibration (^{o}C)

Range	Standard Temperature	Pyrometer Readings
L	1200	1200
H	1300	1306
H	1400	1406
H	1500	1505
H	1600	1605
H	1700	1695
XH	1700	1700
XH	1800	1800
XH	1900	1900
XH	2000	2000
XH	2100	2100
XH	2200	2200

To check the effect of the quartz window on the temperature measurements, the melting points of platinum and rhodium are observed. Platinum (99.9 wt. %) wire 0.081" OD and rhodium (99.9 wt. %) pellets 1/2" OD by 1/16" thick of pressed fine powders supported by

tungsten foil are used as melting point standards. Table 8 permits comparison between the measured temperature and the international scale.

Table 8 Melting Point Standards (^{o}C)

	Melting Points		
Element	IPTS 48	IPTS 68	observed
Pt	1769	1772	1768
Rh	1960	1963	1968

Temperature measurements of the nitride powders are taken by sighting on the blackbody holes (3/64" in diameter, 1/4" deep). No emissivity correction is required[39] and the specimen temperature is taken directly from the pyrometer reading.

The power to the furnace is passively controlled by variable transformers. The power supply delivers constant power. This causes the temperature to drift slowly upward, because the heat shield and furnace interior slowly warms up. Over four hours, the furnace temperature rises 15°C. The temperature at the end of an equilibration is reported as the reaction temperature.

C. Pressure Measurement

Pressures are measured with a mercury-filled U-tube manometer. The pressure readings are converted to mercury density at 0°C. The ID of the tubing is 7/32" and no correction is made for capillary depression. Since the gas pressure is in the viscous flow regime,

---

39. J. Slaughter and J. Margrave in High Temperature Materials and Technology, 1967. Ed. I. Campbell and E. Sherwood. John Wiley and Sons. Page 752.

the pressure at the room temperature manometer is equal to the pressure in the hot reaction zone. Pressures are read to 1 mm and are accurate to ±2 mm.

D. Gas Purity

The nitride metal systems are equilibrated in static nitrogen atmospheres. The chief source of impurity is the desorption of gas from the large mass of graphite heat shields in the furnace. Significant amounts of water and hydrogen are undoubtedly present in the gas phase.

I did not anticipate this in the original design of the experiment. I had planned to work at both high and low pressures. I scratched the low pressure experiments because of potential problems with impurity gases. At the high pressures, nitrogen gas is by far the major gas component and the short mean free path of the high pressure gas limits the diffusion of impurities to the alloys. In section 4H I show that the impurity pick-up is small.

The degassing of the graphite is responsible for a potential health hazard. Carbon and nitrogen can react to form poisonous cyanogen, C_2N_2. In pure nitrogen the extent of reaction is small, but in the presence of hydrogen dangerous amounts of HCN can form.[40] I used a methyl orange-mercuric chloride test for cyanide.[41]

---

40. A.Searcy, Survey of Progress in Chem. 1 (1963) 62.
41. M. Jacobs. The Analytical Toxicity of Industrial Inorganic Poisons, 1967. John Wiley and Sons. Page 726.

The reaction is

$$HgCl_2 + 2\,HClN \rightarrow Hg(CN)_2 + 2\,HCl \qquad (10)$$

Methyl orange changes color in the presence of 2 ppm HCN. No HCN is ever detected.

E. Crucible Interactions

The reactions are carried out without use of crucibles. The alloy is melted in contact with the nitride powder and capillary forces hold the alloy in place. No third phase is close to the reaction interface to act as a source of impurities.

The tungsten liner for the graphite tube reacts only slightly with the system. Tungsten nitrides exist but they only form in the presence of ammonia, and they decompose above 1000°C.[7] Only above 2200°C does the tungsten react with the edge of the pellets, and at 2300°C this reaction is slight after 15 hours.

F. Vaporization

Vaporization is a potential source of problems. At 2327°C platinum has a vapor pressure of 0.14 torr.[42] Its vapor pressure is this value times its activity coefficient. For the similar system Ti-Ir, Pelino[43] has measured $a_{Ir} = 10^{-4}$ at $x_{Ir} = .5$. If platinum has an activity coefficient within an order of magnitude of iridium, its vapor pressure will be 2×10^{-4} torr at most, and its evaporation loss negligible.

---

42. R. Hultgren *et al.*, Selected Values of the Thermodynamic Properties of the Elements, American Society for Metals, Ohio, 1973.
43. M. Pelino, S. Gupta, L. Cornwell and K. Gingerich. J. Less-Common Metals 68 (1979) 31.

G. Activity of Zirconium in ZrN

The equation relating a_{Zr} to free energy and temperature is

$$a_{Zr} = \exp[\Delta G_f^\circ(ZrN)/RT] \tag{11}$$

then the total error in a is

$$\sigma_a = \sqrt{\left(\frac{\partial a}{\partial \Delta G}\right)^2 \delta\Delta G^2 + \left(\frac{\partial a}{\partial T}\right)^2 \delta T^2} \tag{12}$$

Differentiating:

$$\frac{\partial a}{\partial \Delta G} = \frac{a}{RT} \tag{13}$$

$$\frac{\partial a}{\partial T} = -\frac{a\Delta G_f^\circ}{RT^2} \tag{14}$$

and substituting

$$\frac{\sigma_a}{a} = \sqrt{\left(\frac{\delta\Delta G}{RT}\right)^2 + \left(\frac{\Delta G_f^\circ}{R}\right)^2 \left(\frac{\delta T}{T}\right)^4} \tag{15}$$

The difference δ between the free energy of formation of ZrN from thermal data and high temperature equilibrium data is 3 kcal/mole.[44]

For $\delta\Delta G$ = 3 kcal/mole and δT = 10°C

$$\sigma_a = \pm .60a \tag{16}$$

The uncertainty of the activity is large and due mostly to the uncertainty of the free energy.

---

44. C. Alcock, K. Jacob and S. Zador. Atomic Energy Review Special Issue No. 6 (1976). Page 30.

H. Nitride Stoichiometry

The determination and control of the nitride stoichiometry is critical to this study. If z grams of the phase ZrN_{1-x} is converted to y grams of ZrO_2, x can be computed from the equation

$$x = 7.516 - \frac{z}{y} 8.801 \tag{17}$$

The total error in x is

$$\sigma_x = \sqrt{\left(\frac{\partial x}{\partial z}\right)^2 \delta z^2 + \left(\frac{\partial x}{\partial y}\right)^2 \delta y^2} \tag{18}$$

Differentiating

$$\frac{\partial x}{\partial z} = - \frac{8.8}{y} \tag{19}$$

$$\frac{\partial x}{\partial y} = 8.8 \frac{z}{y^2} \tag{20}$$

and substituting

$$\sigma_x = \sqrt{\left(8.8\frac{\delta z}{y}\right)^2 + \left(\frac{8.8z}{y^2}\right)^2 \delta y^2} \tag{21}$$

For a typical nitride,

$y = .595$ g
$z = .5074$ g
$\delta z = .7$ mg
$\delta y = .7$ mg

The computed nonstoichiometry, x, and its error is

$x = .01$ $\qquad\qquad$ $\sigma_x = .01$

I have good control over the nitride stoichiometry; all samples are $Zr_{.51\pm.01}N_{.49\pm.01}$.

I. Alloy Composition

The value of x for Zr_xPt_{1-x} calculated from the weights of Zr and Pt is given by

$$x = g\ Zr \cdot M/91.22 \tag{22}$$

where

$$M = (g\ Zr/91.22 + g\ Pt/195.09)^{-1} \tag{23}$$

The total error in x is

$$\delta x = \pm\sqrt{\left(\frac{\partial x}{\partial g\ Zr}\right)^2(\delta g\ Zr)^2 + \left(\frac{\partial x}{\partial g\ Pt}\right)^2(\delta g\ Pt)^2} \tag{24}$$

Differentiating:

$$\frac{\partial x}{\partial g\ Zr} = \frac{M}{91.22} - g\ Zr\left(\frac{M}{91.22}\right)^2 \tag{25}$$

$$\frac{\partial x}{\partial g\ Pt} = -\frac{g\ Zr}{91.22} \cdot \frac{M^2}{195.09} \tag{26}$$

Substituting

$$\sigma_x = \pm\sqrt{\left(\frac{M}{91.22} - g\ Zr\frac{M}{91.22}\right)^2 \delta g\ Zr^2 + \left(\frac{g\ Zr \cdot M}{91.22 \cdot 195.09}\right)^2 \delta g\ Pt^2} \tag{27}$$

For run 7, I found 11.85 mg Zr and 32.5 mg Pt from an alloy of 4.96 mg. Using the above equations I find

$$x = .42 \qquad \sigma_x = \pm.03$$

VI. RESULTS AND DISCUSSION

Preliminary experiments are performed to optimize the experimental conditions. Zirconium nitride samples with an initial composition of $Zr_{.51}N_{.49}$ are fired at 1750°C in 780 torr of nitrogen for 30 minutes, and 1, 3, and 9 hours. The final composition of all nitrides is $Zr_{.50\pm.01}N_{.50\pm.01}$. The composition is stoichiometric and readily attained.

The choice of the form of the noble metal to use presents difficulties. The experiments with fine powders could not be accurately analyzed. A mixture of 87 volume percent zirconium nitride and 13 volume percent -325 mesh palladium is pressed between two 1.5 gram portions of zirconium nitride. This is fired at 1960°C for 4 hours at 927 torr of nitrogen. The microstructure of the alloy is unusual. At the reaction temperature, the alloy is a liquid. Apparently, it flows around the nitride particles to form a web-like structure. When the alloy cools a solid phase precipitates out and collects in the regions between the nitride particles. The last liquid to solidify forms strands around the nitride. The two phases of this alloy have segregated into different regions. It is difficult to accurately analyze the mole fraction of each alloy in the original liquid. This precludes the use of a microprobe for sample analysis.

A second experiment is made with .002" thick platinum foil. Because this foil is thin and the diffusion distances small, attainment of equilibrium will be promoted. The specimen is fired at 1815°C for 1.5 hours under 876 torr of nitrogen. The reaction product is unsatisfactory on two counts: (1) it has a mysterious

microstructure, containing many voids (Figure 8) and (2) there is insufficient sample for an accurate chemical analysis. The voids may have an innocent origin; they could form if on melting the liquid platinum is drawn into voids in the nitride phase. Still this strange microstructure makes this alloy suspect.

Being unable to obtain sufficient sample from the powder or thin foils to do a chemical analysis, I try a third experiment with .01" thick platinum. The platinum disc is embedded in zirconium nitride and equilibrated at 2045°C for 3 hours. Its microstructure is shown in Figure 12. The disc has separated into two sections and some single phase liquid has collected between the layers. Undoubtably chemical equilibrium is obtained at these high temperatures in a liquid because diffusion rates are so high. On cooling, different phases form and segregate into different regions. This segregation makes a microprobe analysis inaccurate. Therefore, the total sample must be chemically analyzed. Unfortunately, most of the alloy in this sample is consumed in microstructure characterization.

The fourth experiment is an attempt to duplicate the results of Brewer and Wengert. A platinum disc .01" in thickness is embedded in zirconium nitride and equilibrated at 1670°C for 3 hours under 758 torr of nitrogen. The activity of zirconium is 1×10^{-5} under these conditions. The chemical composition of the alloy is determined to be $Zr_{.26\pm.03}Pt_{.79\pm.03}$. Wengert found $Zr_{.25}Pt_{.75}$ as his reaction product under similar conditions, at a temperature of 1527°C and zirconium activity of 5×10^{-6}.

Figure 12.
Alloy Cross-Section (Magnification 140x, 1" = 180 microns)

Fig. 12

XBB805 6421

To determine whether the sample reached equilibrium, a fifth experiment is performed at a slightly higher temperature (1735°C) and for a longer time (9 hours). At a pressure of 839 torr, the activity of zirconium is $2\pm1 \times 10^{-5}$. The composition of the alloy is determined to be $Zr_{.35}Pt_{.65}$. This cannot be the equilibrium product. Figure 8 shows a polished cross-section of the alloy. The top layer in the photograph is a two phase zirconium platinum alloy and the bottom layer is the zirconium nitride. The alloy section contains two phases, the composition $Zr_{.35}Pt_{.65}$ corresponds to a mixture of equal mole fractions of $ZrPt_3$ and Zr_7Pt_{10}.

At the reaction temperature, a two phase alloy is unlikely to be the equilibrium reaction product. The zirconium activity is fixed by the temperature and gas pressure. The equilibrium product will have this same zirconium activity. A single phase region is stable over a range of zirconium activities. For example, the phase PdAl is stable with activities of aluminum ranging from 10^{-4} to 0.5.[45]

In contrast, a two phase alloy can have only one zirconium activity at fixed temperature and pressure. Varying the mole fractions of the mixture does not affect the zirconium activity. In order to have a two phase alloy in equilibrium with the alloy, the temperature and pressure must be exactly matched. This condition is unlikely to exist. The alloy composition must then be kinetically controlled and not thermodynamically determined. Zirconium diffuses into the alloy and forms $ZrPt_3$. This phase then undergoes further reaction to form Zr_7Pt_{10}, but apparently this process is slow at

1720°C. The results of the first run then must also be diffusion limited. Only because the reaction is at a lower temperature and the diffusion coefficients are smaller does the reaction stop at $ZrPt_3$.

A sixth run is made with a high concentration zircon um alloy as the starting material. An experiment with high concentration alloys is vital to this work. Only if the sample composition is reached from both high and low concentration of zirconium is equilibrium certain to be achieved. A .008" thick slice of $Zr_{.6}Pt_{.4}$ is equilibrated at 735°C for 4 hours. Under 817 torr of nitrogen, the zirconium activity is 1.95×10^{-5}. The alloy reaction product is found to be $Zr_{.49\pm.01}Pt_{.51\pm.01}$. This is a homogeneous phase, but this alone does not insure it is the equilibrium phase.

A seventh experiment is made at high temperature to eliminate diffusion problems. A .01" thick Pt disc is equilibrated with zirconium nitride at 2045°C for 2.5 hours. At a pressure of 518 torr of nitrogen, the zirconium activity is 5×10^{-4}. The composition is analyzed and found to be $Zr_{.42\pm.03}Pt_{.58\pm.03}$. Figure 7 is a micro-photograph of the reaction product. The top area is the bakelite mounting material, the middle layer is the two-phase alloy reaction product, and the bottom area of the picture shows the zirconium nitride phase. The existence of two phases in the alloy does not imply equilibrium has not been attained. At the reaction temperature, the phase diagram is not well established; $Zr_{.42}Pt_{.58}$ is either a

---

45. M. Ettenberg, K. L. Komarek and E. Miller, Met. Trans. 2 (1971) 1173.

liquid or within 15°C of a liquid-solid region. Kendall *et al.* [11] report a liquid at 2000°C with this composition. On cooling and solidification, two solid phases, Zr_7Pt_{10} and Zr_9Pt_{11} in the mole fractions 78% and 22% respectively would form. The two solid phases are probably the result of a single phase liquid alloy.

A final run with zirconium platinum alloys yields conclusive results. Two pellets, one with .01" thick Pt and the other with .012" thick $Zr_{.6}Pt_{.4}$ are heated at 1985°C for 8 hours under 792 torr of nitrogen. The activity of zirconium is 2.4×10^{-4}. The reaction product of the pure platinum sample is $Zr_{.44\pm.03}Pt_{.56\pm.03}$ and of the zirconium platinum alloy $Zr_{.45}Pt_{.55}$. This corresponds to the single phase Zr_9Pt_{11}. The attainment of the same end product by both high and low zirconium content alloys is convincing proof that equilibrium has been reached.

The limit on the free energy of formation of this alloy is computed. Since the reaction

$$ZrN + \frac{11}{9} Pt \rightarrow \frac{1}{9} Zr_9Pt_{11} \qquad (28)$$

proceeds spontaneously ($\Delta G^\circ < 0$), The free energy change for the reaction is

$$\Delta G^\circ = \frac{1}{9} \Delta G_f^\circ(Zr_9Pt_{11}) - \Delta G_f^\circ(ZrN) \qquad (29)$$

Since

$$\Delta G^\circ_{f,1985^\circ C}(ZrN) = -36{,}900 \text{ kcal/mole}$$

then

$$\Delta G^{\circ}_{f,1985^{\circ}C}(Zr_9Pt_{11}) \leq -16.6 \text{ kcal/mole.}$$

As predicted by the Engel-Brewer Theory, the free energy of zirconium platinum is large and negative.

To further explore the role of electronic configuration, experiments are performed on iridium-zirconium and iridium-platinum-zirconium systems. Iridium discs 7/32" OD and .02" thick are embedded in zirconium nitride. The pellet is heated at 2330°C for 15 hours. I am unable to analyze the reaction product. No acid that I use can dissolve the zirconium iridium alloy. Alloys of composition $Ir_{.38}Pt_{.62}$ and $Ir_{.17}Pt_{.83}$ are made and equilibrated with zirconium nitride. The reaction product of the $Ir_{.38}Pt_{.62}$ alloy could only be partially dissolved. About 30 weight percent of the alloy remained undissolved. Platinum 0.3 mole fraction iridium alloys are resistant to even fused alkalies.[46] Perhaps the reaction alloy is a non-equilibrium two phase alloy, one of whose components is insoluble in the acids I used.

I am able to determine the reaction product of the $Ir_{.17}Pt_{.83}$ alloy. A .015" thick slice of $Ir_{.17}Pt_{.83}$ is equilibrated first at 1850°C for 8.5 hours under 584 torr of nitrogen and then at 2190°C for 4 hours under 948 torr of nitrogen. The activity of zirconium in the last heating is 1.2×10^{-3}. The product composition is $Zr_{.37}(Ir_{.17}Pt_{.83})_{.63}$ (assuming no evaporation loss of platinum).

---

46. Werner Espe, Materials of High Vacuum Technology. Pergammon Press, Oxford, 1966. Volume 1, page 168.

Since the iridium alloy melts at 1825°C and the equilibration temperature is 2190°C, this is likely to be the equilibrium alloy composition. The computed free energy of formation for this phase is

$$\Delta G_f^\circ(Zr_{.37}Ir_{.11}Pt_{.52}) \leq -16.0 \text{ kcal/mole}$$

Experiments are performed with zirconium-molybdenum, zirconium-tungsten, and combinations of these metals with platinum. Table 9 gives the conditions of reaction and the results.

Table 9

Metal (thickness) reacted with ZrN	Temperature (°C)	Time (hrs.)	P_{N_2} (torr)	Product
Mo (.01")	1815	2	760	.01 Zr
W (.01")	2300	15	932	.01 Zr
$W_{.1}Pt_{.9}$ (.008")	2250	10	906	?
$W_{.26}Pt_{.74}$ (.006")	2250	10	906	?
$Mo_{.11}Pt_{.89}$ (.012")	2250	10	906	?

An X-ray flourescence study of this sample could detect no zirconium in the metal at a sensitivity of 1 atomic percent. Similarly no zirconium could be detected in the tungsten. These results are undoubtedly kinetically limited. The temperature of reaction is too far below the melting points of these metals to promote fast diffusion. The King furnace can operate to 3000°C but the power supply can deliver only enough power for operation to 2300°C.

My analytical procedures failed for the chemical analysis of the platinum tungsten alloys. I am not able to obtain self-consistent results. Hydrous tungsten oxides form which remove much of the zirconium from solution. This is unfortunate, for the platinum tungsten system is an excellent test for Brewer's theory of Lewis acid-base interactions. Metallic solutions are difficult to study by an inductive technique because as the alloy composition changes, its structure can also change. Platinum-tungsten alloys have the same structure from 40 to 100 atomic percent platinum. Changes in their properties with composition are the result of valence and not structure effects. Comparing the stability of zirconium in $Pt_{.5}W_{.5}$ (electronic configuration d^6sp) with zirconium in Ir (electronic configuration d^6sp^2) would help fix the role of s and p electrons in phase stability.

The last portion of this section will be a discussion of preliminary experiments on silicon-platinum-zirconium alloys.

Vaporization losses from high-temperature platinum-silicon alloys are small. Searcy and Finnie[47] have measured the activity of silicon in PtSi. They report an activity coefficient of .05. The vapor pressure of silicon for $Pt_{.9}Si$ is computed to be.5 millimicrons at 1750°C.

Phase compatibility experiments are performed with Si_3N_4 and ZrN. Pellets of intimately mixed powders of Si_3N_4 and ZrN are fired at 1740°C

---

47. A. Searcy and L. Finnie, J. Am. Ceram. Soc. 45 (1962) 268.

for 3 hr. Porous bodies result containing many dark specks. The X-ray diffraction pattern of the fired pellet shows only ZrN lines. Presumably the two nitrides react to form a silicon-zirconium alloy, but in amounts too small to be detected. ZrN should be the equilibrium in contact with Si-Pt-Zr alloys; a ternary Si-Zr-N phase does not form.[28]

The final experiment was conducted with alloys of composition $Si_{.1}Pt_{.9}$ and $Si_{.19}Pt_{.81}$ and thicknesses 0.012" and 0.015" are equilibrated at 1750°C for 6 hrs in 814 torr of nitrogen. The alloy compositions are $Zr_{.46\pm.04}(Si_{.1}Pt_{.9})_{.54\pm.04}$ and $Zr_{.57\pm.02}(Pt_{.81}Si_{.19})_{.43\pm.02}$, assuming no silicon loss. Silicon with its large affinity for zirconium acts to increase its solubility in platinum.

VII. CONCLUSIONS and SUGGESTIONS FOR FUTURE WORK

These results conclusively resolve the conflict between the work of Meschter and Wengert. Wengert worked with fine platinum powders equilibrated at 1600°C for 3 hr. The results presented in this paper demonstrate that $ZrPt_3$, the reaction product formed, is not the equilibrium alloy at 1600°C. Higher temperatures are needed to promote diffusion through the high melting intermetallic compounds of the zirconium-platinum system. Wengert's reactions do not form the high zirconium concentration alloy for kinetic and not thermodynamic reasons. Meschter uses an emf technique which does not rely on gross mass transfer.

Results are presented in this paper for the activity of zirconium in Zr_9Pt_{11}. The reaction conditions are well-characterized. The results of this investigation are $a_{Zr}^{1985^oC} = 2.4\times10^{-4}$ in Zr_9Pt_{11} and $\Delta G^o_{f,1985^oC}$ $Zr_9Pt_{11} \leq -16.6$ kcal/ g atom.

The techniques used for this study can be adapted to alloys of group 3,4,5 transition metals, boron, aluminum and silicon with platinum group metals. Brewer's model predicts a maximum stability of MePt for Me=Hf. Tantalum, hafnium and lanthanum can be studied by nitride equilibria to verify this prediction.

Aluminum and silicon alloyed with platinum group metals are of interest. Platinum is used as an electrical contact in semiconductor devices. The formation of a low melting, platinum-silicon alloy is a potential cause of device failure in production. Platinum catalysts are often supported on alumina substrates. Thermodynamic data for aluminum-platinum alloys would allow process designers to avoid conditions that result in substrate-catalyst side reactions.

The study of select ternary alloy systems would be a great aid in the development of bonding models. The electronic configuration in these alloys could be precisely controlled. These alloys hold promise for interesting results, but they are experimentally difficult to work with.

Material Suppliers

The materials and their suppliers are listed below. The zirconium nitride and zirconium metal are products of Cerac, Inc., which provided an elemental analysis. Platinum, iridium, tungsten, and molybdenum are from Lawrence Berkeley Laboratory (L.B.L.) stock. The silicon is a product of Matheson, Coleman and Bell. The chemical analysis of the materials is given in Table 4.1.1. The analysis for zirconium nitride and zirconium is given by the manufacturer, the rest were analyzed by American Spectrographic Laboratories, San Francisco, CA.

Table 4.1.1 Raw Materials

Zirconium nitride, 99%, Cerac (*weight percent*)

Zr	86.96	Fe	.3	Pb	.1	Nb	1	Mg	.03
N	12.5	Al	.1	Ta	.2	Hf	.06	Ni	.04
C	.31	Si	.04	Ti	.03	Cr	.02		

Platinum, 99.9%, L.B.L. stock (*weight percent*)

Pd	.02	Cu	.004
Rh	.02	Ca	<.001
Au	<.01		

Zirconium metal, 99.8%, Cerac (*weight percent*)

C	.0140	Fe	.0325	Nb	.0100
N	.0021	Al	.0120	Hf	.056
Cl	.0100	Ta	.0200		

Iridium, L.B.L. stock (*weight percent*)

Rh	.2	Cu	<.002
Pt	.02	Ca	<.001
	.015	Fe	.01

Tungsten, Molybdenum, L.B.L. stock

No impurities noted by spectrographic analysis.

Si, silicon lumps, Matheson, Coleman and Bell (*weight percent*)

Fe	.4	Mn	.05	Mg	.006	Ni	.002
Al	.25	Ca	.02	Zr	.004	Ba	.001
Ti	.05	Cr	.015	Cu	.003		